The Spectrum of the FeLoBAL Quasar FBQS 1214+2803: A Resonance–Scattering Interpretation

David Branch, Karen M. Leighly, R. C. Thomas, and E. Baron

Department of Physics and Astronomy, University of Oklahoma, Norman, Oklahoma 73019, USA

ABSTRACT

The usual interpretation of the spectrum of a BALQSO is that a broad–band continuum from the central engine plus broad emission lines from a surrounding region (the BELR) emerges from near the center of the QSO, and broad absorption lines are superimposed in a separate outlying region (the BALR). For FBQS 1214+2803, designated as an FeLoBAL QSO because its spectrum contains numerous absorption features from excited states of Fe II, we explore an alternative interpretation based on resonance scattering. In this model line emission and absorption occur in the same line–forming region (the LFR). A resonance–scattering synthetic spectrum computed with the parameterized supernova synthetic–spectrum code SYNOW fits the spectrum of FBQS 1214+2803 rather well, so the resonance–scattering model merits further study. Some implications of the model and its possible applicability to other QSOs are briefly discussed.

Subject headings: quasars: absorption lines – quasars: individual (FBQS 1214+2803) — radiative transfer

1. INTRODUCTION

BALQSOs — quasars that have broad absorption lines in their spectra — can be divided into LoBALs and HiBALs, which do and do not have strong absorption lines produced by low–ionization species such as Mg II, Al III, and Fe II. LoBALs that have numerous lines from excited states of Fe II are called FeLoBALs (Becker et al. 1997, 2000).

The usual interpretation of the spectrum of an FeLoBAL QSO is similar to that of the spectra of other BALQSOs. The effective continuous spectrum consists of a true continuum from the accretion disk, plus broad emission lines (BELs) that form in a surrounding region — the BELR. Broad absorption lines (BALs) are superimposed on the effective continuum

as it passes through a separate region — the BALR. The distance of the BALR from the QSO center may be large compared to the size of the BELR, and the global covering factor — the fraction of the sky covered by the BALR as viewed from the center of the QSO — may be small.

In this *Letter* we explore an alternative interpretation of the spectrum of a particular FeLoBAL QSO. In our simple model, the rest–frame UV spectrum consists of P Cygni features formed by resonance scattering, superimposed on a continuum. The line emission and absorption components come from the same spherically–symmetric line–forming region — the LFR. To illustrate this interpretation we concentrate on an FeLoBAL that was discovered in the First Bright Quasar Survey (White et al. 2000) and is designated FIRST J121442.3+280329, or FBQS 1214+2803 for short. We choose this particular FeLoBAL because it has recently been analyzed in detail, in the context of the usual BAL model, by de Kool et al. (2002; hereafter dK02), and because its spectrum, although rich in lines, appears to be amenable to an analysis based on a single LFR. In §2 we describe the modeling of FBQS 1214+2803 by dK02. The alternative resonance–scattering interpretation is presented in §3. Some of the implications of the resonance–scattering model, and its possible applicability to other QSOs, are briefly discussed in §4.

2. A RECENT INTERPRETATION OF THE SPECTRUM OF FBQS 1214+2803

Because we make use of the results of dK02, and we want to compare and contrast the results of our model and theirs, we must first briefly describe their analysis. They studied a spectrum obtained on 1998 May 18 using the High Resolution Echelle Spectrometer (HIRES; Vogt et al. 1994) on the Keck I 10 m telescope. The redshift was determined to be $z = 0.692$.

In their analysis dK02 used effective continuous spectra that consisted of a power–law continuum plus Fe II and Mg II BELs. The Mg II BEL was the sum of two Gaussians centered on the two components of the Mg II λ2798 doublet ($\lambda\lambda$2796, 2803). Two different templates for the Fe II BELs were considered. The first consisted of a linear combination of five sets of Fe II BELs from theoretical model calculations (Verner et al. 1999), and the second was the observed Fe II BEL spectrum of the strong emission–line QSO 2226–3905 (Graham, Clowes, & Campusano 1996).

For the absorption features, dK02 obtained a template distribution of line optical depth with respect to velocity in the BALR from the observed absorption profile of Fe II λ3004, an apparently unblended line of moderate strength. Given the assumption that only absorption

takes place in the BALR, the optical depth was obtained from $\tau(v) = -ln\ F_\lambda$, where F_λ is the fractional residual flux in the absorption feature. The resulting optical–depth distribution extended from about 1200 to 2700 km s^{-1} and peaked near 2100 km s^{-1}. This optical–depth distribution, scaled in amplitude, was used for all absorption lines. For each of the absorbing ions that were introduced — Fe II, Mg II, Cr II, and Mn II — the column density was a fitting parameter. The relative strengths of the lines of each ion turned out to be consistent with LTE.

Three models that differed in their details (see dK02) were presented, with similar results. The column densities of Fe II, Cr II, and Mn II were well constrained. (The column density of Mg II could not be well constrained because the only Mg II absorption, due to λ2798, is saturated.) The excitation temperature was found to be near 10,000 K. Two local covering factors, representing the fractions of the power–law source and the BELR that are covered by the BALR as viewed by the observer, were introduced to reproduce the observed "non–black saturation" — the fact that in the observed spectrum even very strong absorption features do not go to zero flux. Both local covering factors were found to be 0.7 ± 0.1.

A detailed view of the spectral fit for one of the models was presented, and practically all of the observed absorptions were reasonably well accounted for. To further interpret the results of their spectrum fits dK02 then used the photoionization–equilibrium code CLOUDY (Ferland 2000) to compute a grid of constant–density slab models irradiated by a range of ionizing spectra. The ionization parameter U, the hydrogen density n_H, and the hydrogen column density N_H were found to satisfy $-2.0 < log\ U < -0.7$, $7.5 < log\ n_H < 9.5$, and $21.4 < log\ N_H < 22.2$. From these values the distance of the BALR from the center of the QSO was inferred to be between 1 and 30 pc.

3. A RESONANCE–SCATTERING INTERPRETATION

We explore a resonance-scattering interpretation using synthetic spectra generated with the fast, parameterized synthetic–spectrum code SYNOW, which often is used for making line identifications and initial coarse analyses of photospheric–phase supernova spectra. The use of SYNOW, as well as more elaborate and physically self–consistent spectrum–synthesis codes such as PHOENIX, for the analysis of supernova spectra is reviewed by Branch, Baron, & Jeffery (2002). SYNOW assumes spherical symmetry and a sharp photosphere that emits a blackbody continuum characterized by temperature T_{bb}. Expansion velocity is proportional to radius, as expected for matter that has been coasting at constant velocity after an impulsive ejection with a range of velocities. Line formation, treated in the Sobolev approximation, occurs by resonance scattering of photons from the photosphere. Line blending (multiple

scattering) is treated exactly, within the context of the Sobolev approximation. Line optical depths are taken to decrease with radius according to a power law. For each ion whose lines are introduced, the optical depth of a "reference line" at the inner boundary of the LFR is a fitting parameter, and the optical depths of the other lines of the ion are determined by assuming LTE level populations at excitation temperature T_{exc}. Oscillator strengths are from Kurucz (1993). In supernovae, line formation ordinarily takes place immediately above the photosphere, i.e., the bottom of the LFR has the velocity at the photosphere, v_{phot}, but sometimes it is appropriate to "detach" the lines of an ion by allowing line formation only above some velocity v_{min} that exceeds v_{phot}. Individual values of v_{min}, and also of v_{max}, can be assigned to each ion.

For FBQS 1214+2803 we use $T_{bb} = 8000$ K to approximate the shape of the underlying continuum, we take $T_{exc} = 10,000$ K from the analysis of dK02, and we introduce only lines of Mg II, Fe II, and Cr II. (In the synthetic spectrum of dK02 the Mn II lines play only a minor role.) The index of the optical–depth power law is taken to be $n = 2$ for all ions.

Fig. 1 compares the strong observed feature produced by Mg II λ2798 with a synthetic spectrum that contains only lines of Mg II and has $v_{phot} = 1000$ km s^{-1}, $v_{max} = 2800$ km s^{-1}. The synthetic P Cygni profile is so saturated that it not sensitive to the optical depth distribution, only to the values of v_{phot} and v_{max}. It is interesting that the observed feature can be fit this well with the simple assumption of resonance scattering in a spherically symmetric LFR. Note that no local covering factor has had to be introduced; because line emission and absorption take place in the same LFR, the saturated absorption feature does not go black.

Fig. 2 compares the spectrum of FBQS 1214+2803 with a synthetic spectrum that contains lines of Mg II, Fe II, and Cr II, all with $v_{max} = 2800$ km s^{-1}. In order to make their absorption components blueshifted enough, the Fe II and Cr II lines have $v_{min} = 1800$ km s^{-1}. Cr II and Fe II contribute some lines of weak and moderate strength to the right of the Mg II feature, while Fe II lines dominate the spectrum to the left of the Mg II feature. The overall fit is good, although there are some discrepancies. The fact that the synthetic continuum goes too high at the red end of the spectrum is not a serious concern because there is no reason that the true continuum should be that of a blackbody. The strong Fe II blends near 2740, 2620, and 2400 Å are reasonably well matched, although now that the Mg II feature is blended with numerous Fe II lines it does not fit as well as in Fig. 1. The Cr II absorption to the right of the Mg II emission is too strong. A closer look at a crowded part of the spectrum (Fig. 3) shows that most of the details are fit rather well, considering the simplicity of our model and especially that we are using a power–law optical–depth distribution rather than a customized (template) distribution of optical depth with respect to velocity. Why do the

Fe II and Cr II features form only above 1800 km s^{-1} while Mg II forms above 1000 km s^{-1}? The simplest possibility is that the true optical–depth distributions of Mg II, Fe II, and Cr II lines with respect to velocity are of similar shape, but their relative amplitudes are such that the optical depths of the Fe II and Cr II lines are less than unity below 1800 km s^{-1} while the optical depth of the very strong Mg II resonance feature is well above unity.

An extension of the synthetic spectrum of Fig 2. to longer wavelengths is practically featureless. For anything like solar abundances, the only lines in the rest–frame optical spectrum that necessarily should be expected in this model are the hydrogen lines, although some lines of other ions that we have not used for the UV spectrum, such as the H&K lines of Ca II, might have significant optical depths. An extension of the synthetic spectrum of Fig. 2 to wavelengths shorter than 2300 Å has numerous features of moderate strength, and strong features also are to be expected from ions such as Al III and Al II that are not needed for Fig. 2.

4. DISCUSSION

The resonance–scattering model can fit the spectrum of FBQS 1214+2803 rather well with simple assumptions, and if we were to introduce a customized distribution of optical depth with respect to velocity the fit certainly could be improved. Nevertheless, the model is at best an idealization, and it needs more study before we can be sure that it is applicable. Our use of an $n = 2$ power law for the optical depths is just illustrative because here a power–law has no particular justification; the 8000 K blackbody continuum is just a surrogate for the real continuum from the central source; and our assumption that velocity is proportional to distance from the center may not be correct. The most important feature of this model is that the red side of the emission component comes from the far side of the QSO rather from a central BELR, so it would mean that the LFR is more or less spherically symmetric and continuous and the global covering factor is large. Since emission and absorption components come from the same LFR, the fact that the same lines are observed in emission and absorption would necessarily follow. Local covering factors would not necessarily be required to account for non–black saturation. For lines of more than moderate strength, column densities inferred from the resonance scattering intepretation would be higher than those inferred from the standard model because with the presence of emission in the LFR, larger optical depths would be required to match a given absorption depth in the observed spectrum. Thus the excitation temperature inferred from a detailed line by line study could change.

Taking $M_B = -26.3$ from Becker et al. (2000) and assuming a standard AGN spectral energy distribution (Mathews & Ferland 1987) we estimate the luminosity of FBQS 1214+2803

to be roughly 6×10^{46} erg s^{-1}. If, for example, the luminosity is ten percent of the Eddington luminosity then the black–hole mass is 5×10^9 M$_\odot$, and the escape velocity falls to 1000 km s^{-1} at a radius near 20 pc. If the inner radius of the LFR is at least this large, then the LFR does not contain a true photosphere, because a blackbody having $T = 8000$ K and $L = 6 \times 10^{46}$ erg s^{-1} would have a radius of only 1.4×10^{17} cm, or 0.045 pc. The column density of singly ionized iron required to produce the weak Fe II lines is 10^{17} cm^{-2} (dK02), which with a solar iron abundance and *all* iron being singly ionized corresponds to a bare minimum hydrogen column density of $10^{21.4}$ cm^{-2}. On the other hand, if the LFR is optically thick to electron scattering the column density exceeds 10^{24} cm^{-2}. Then the mass of the LFR could be large, $6 \times 10^7 r_{20}^2 N_{24}$ M$_\odot$, where r_{20} is the inner radius of the shell in units of 20 pc and N_{24} is the column density in units of 10^{24} cm^{-2}.

The kinetic–energy luminosity of $\sim 10^{45} r_{20} N_{24}$ erg s^{-1} is not necessarily large compared to the QSO luminosity but the mass flow rate of $\sim 3000 r_{20} N_{24}$ M$_\odot$ y^{-1} may be large compared to the accretion rate required to provide the QSO luminosity (~ 10 M$_\odot$ y^{-1}, if the efficiency of conversion of accretion energy to radiation is ten percent), in which case the LFR is a consequence not of a steady–state wind but an episodic ejection.

Resonance scattering in differentially expanding LFRs having high global covering factors was explored years ago (e.g., Scargle, Caroff, & Noerdlinger 1970; Surdej & Swings 1981; Drew & Giddings 1982, Surdej & Hutsemékers 1987) but it fell out of favor as a model for BALQSOs in general, for various reasons. Weymann et al. (1991) found that HiBALs and non–BALQSOS have similar emission lines, suggestive of a single population of QSOs having a small global covering factor, with HiBALs being seen from a special orientation. Emission–line equivalent widths often are too small to account for the photons scattered out of the deep absorption troughs (barring some photon destruction mechanism, e.g., absorption by dust); from analysis of emission and absorption line profiles Hamann, Korista & Morris (1993) concluded that high global covering fractions were not favored for the HiBALs of the Weymann et al. sample. However, Becker et al. (2000) and Gregg et al. (2002) have argued against the usual scenario that BALQSOs are normal quasars seen edge–on, and in favor of an alternative picture in which BALQSOs are an early stage in the development of new or refueled quasars. (Evolution, not orientation.)

We suggest that the resonance–scattering model should be reconsidered, for the FeLoBAL QSOs. Our preliminary modeling of the spectra of FeLoBALs other than FBQS 1214+2803 indicates that the resonant–scattering model is able to account for the spectra of at least some of them.

Although the model clearly is not applicable to all BALQSOs, it may have some relevance to LoBAL QSOs in general. LoBALs have different emission–line properties from

HiBALs, including a small equivalent width of [O III] λ5007 (Boroson & Meyers 1992). The [O III] line is produced far enough from the center of the QSO that its emission should be isotropic (Kuraszkiewicz et al. 2000), therefore a small equivalent width may imply a high global covering factor (e.g., Boroson & Green 1992). Large column densities and global covering factors may alleviate the current discrepancy between UV and X-ray column densities. Green et al. (2001) found that LoBALs are weaker X-ray sources than HiBALs, implying higher column densities for LoBALs. Other evidence that has been cited for high column densities includes reddened optical and UV spectra (Sprayberry & Foltz 1992; Boroson & Meyers 1992; Egami et al.1996; Brotherton et al. 2001) and large Balmer decrements (Egami et al. 1996).

As mentioned above, if the mass outflow rates are too high to be maintained in steady–state, the outflows may originate from episodic ejections, perhaps associated with the turning on of QSOs (Hazard et al. 1984). LoBALs may be young quasars in the act of casting off their cocoons of gas and dust (Voit et al. 1993), related to ultraluminous infrared galaxies (Egami 1999). Becker et al. (1997) suggest that FeLoBALs may be the missing link between galaxies and quasars.

It appears that for some QSOs the simple SYNOW code may be useful for making rapid explorations and gaining some insight. However, we have merely characterized the LFR without explaining how it is heated, and we have ignored the implication from the observed spectropolarization of FeLoBALs (Brotherton et al. 1997; Hutsemékers, Lamy, & Remy 1998; Schmidt & Hines 1999; Lamy & Hutsemékers 2000) that not all components can be spherically symmetric. Detailed physically self–consistent calculations with more powerful synthetic–spectrum codes such as PHOENIX must be the basis for ultimate decisions about the viability of the model sketched here. We intend to undertake such calculations for FeLoBALs.

We are grateful to Bob Becker for providing the spectrum of FBQS 1214+2803 and to Jules Halpern and an anonymous referee for constructive comments. This work has been supported by National Science Foundation grants AST–9986965 and AST–9731450 and by NASA grant NAGS–10171.

REFERENCES

Becker, R. H., Gregg, M. D., Hook, I. M., McMahon, R. G., White, R. L., & Helfand, D. J. 1997, ApJ, 479, L93

Becker, R. H., White, R. L., Gree, M. D., Brotherton, M. S., Laurent–Muehleisen, S. A., & Arav, N. 2000, ApJ, 538, 72

Boroson, T. A., 2002, ApJ, 565, 78

Boroson, T., & Green, R.., 1992, ApJS, 80, 109

Boroson, T. A., & Meyers, K. A., 1992, ApJ, 397, 442

Branch, D., Baron, E., & Jeffery, D. J., in Supernovae and Gamma–Ray Bursts, ed. K. W. Weiler (New York: Springer–Verlag), in press (2002); astro-ph/0111573

Brotherton, M. S., Tran, H. D., van Breugel, W., Dey, A., & Antonucci, R., 1997, ApJL, 487, 113

Brotherton, M., S., Tran, H. D., Becker, R. H., Gregg, M. D., Laurent-Muehliesen, S. A., & White, R. L., 2001, ApJ, 546, 775

de Kool, M., Becker, R. H., Gregg, M. D., White, R. L., & Arav, N. 2002, ApJ, 567, 58

Drew, J., & Giddings, J. 1982, MNRAS, 201, 27

Egami, E., 1999, in Proc. "Galaxy Interactions at Low and High Redshift", eds. J. E. Barnes and D. B. Sanders (IAU), 475

Egami, E., Iwamuro, F., Maihara, T., Oya, S., & Cowie, L. L., 1996, AJ, 112, 73

Ferland, G. J. 2000, Hazy, A Brief Introduction to Cloudy 94.00 (Univ. Kentucky)

Graham, M. J., Clowes, R. G., & Campusano, L. E. 1996, MNRAS, 279, 1349

Green, P. J., Aldcroft, T. L., Mathur, S., Wiles, B. J., & Elvis, M. 2001, ApJ, 558, 109

Gregg, M. D., Becker, R. H., White, R. L., Richards, G. T., Chaffee, F. H., & Fan, X. 2002, ApJL, 573, L85

Hamann, F., Korista, K. T., & Morris, S. L., 1993, ApJ, 415, 541

Hazard, C., Morton, D. C., Terlevich, R., & McMahon, R., 1984, ApJ, 282, 33

Hutsemékers, D., Lamy, H., & Remy, M., 1998, A&A, 340, 371

Kuraszkiewicz, J., Wilkes, B. J., Brandt, W. N., & Vestergaard, M., 2000, ApJ, 542, 631

Kurucz, R. L. 1993, CD-ROM 1, Atomic Data for Opacity Calculations (Cambridge: Smithsonian Astrophysical Observatory)

Lamy, H., & Hutsemékers, D., 2000, A&A, 356, L9

Mathews, W. G., & Ferland, G. J. 1987, ApJ, 323, 456

Scargle, J. D., Caroff, L. J., & Noerdlinger, P. D. 1970, ApJ, 161, L115

Schmidt, G. D., & Hines, D. C., 1999, ApJ, 512, 125

Sprayberry, D., & Foltz, C. B. 1992, ApJ, 390, 39

Surdej, J., & Hutsemékers, D. 1987, A&A, 177, 42

Surdej, J., & Swings, J. P. 1981, A&A, 96, 242

Verner, E. M., Verner, D. A., Korista, K. T., Ferguson, J. W., Hamann, F., & Ferland, G. J. 1999, ApJS, 120, 101

Voit, G. M., Weymann, R. J., & Korsta, K. T. 1993, ApJ, 413, 95

Vogt, S. S., et al. 1994, Proc. SPIE, 2198, 362

Weymann, R. J., Morris, S. L., Foltz, C. B., & Hewitt, P. C. 1991, ApJ, 373, 23

White, R. L. et al. 2000, ApJS, 126, 133

AAS LaTeX macros v5.0.

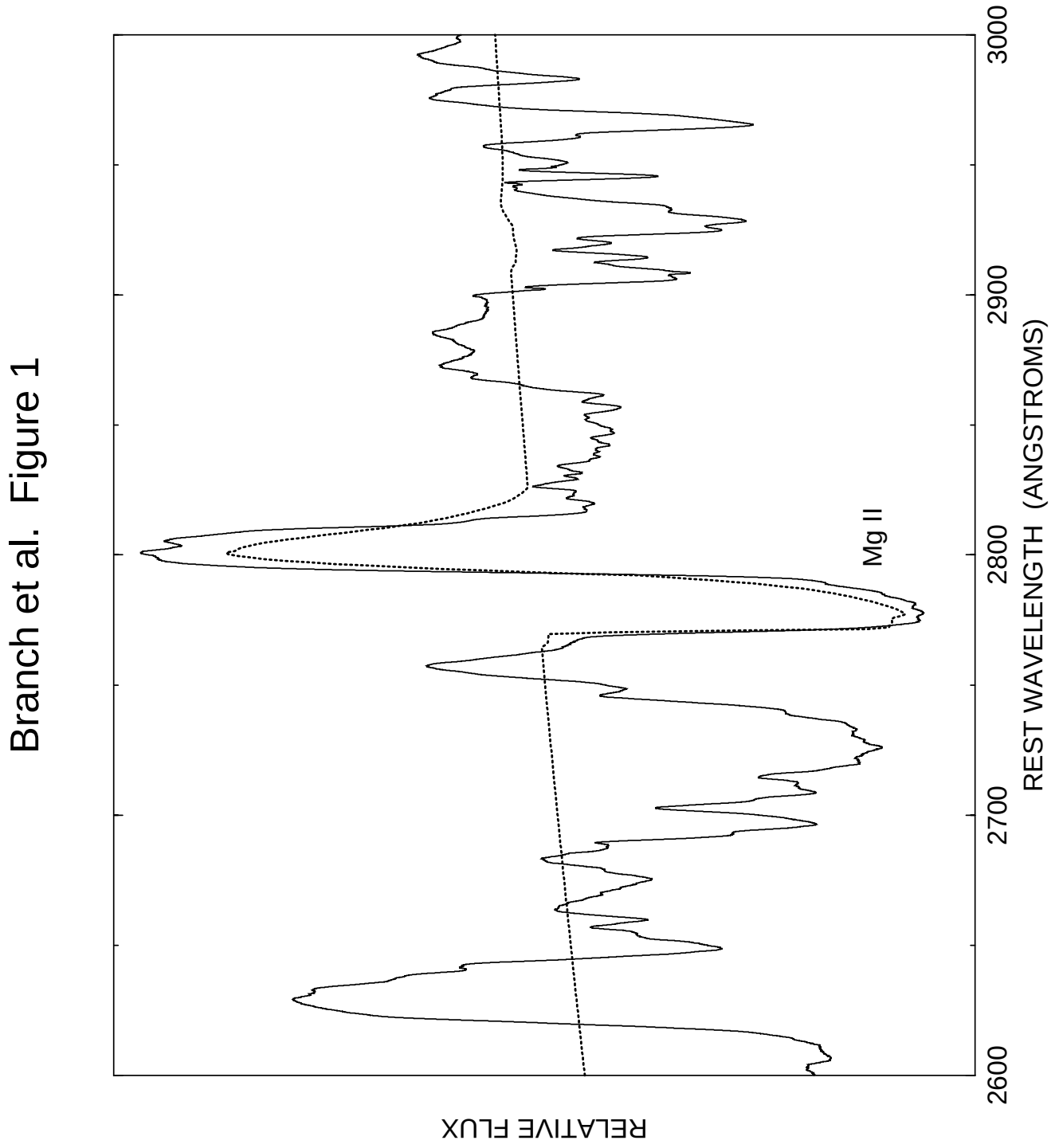

Fig. 1.— The spectrum of FBQS 1214+2803 in the region of the Mg II λ2798 feature (*solid line*) is compared with a resonance–scattering synthetic spectrum (*dotted line*) that contains only lines of Mg II and has $v_{min} = 1000$ km s^{-1} and $v_{max} = 2800$ km s^{-1}.

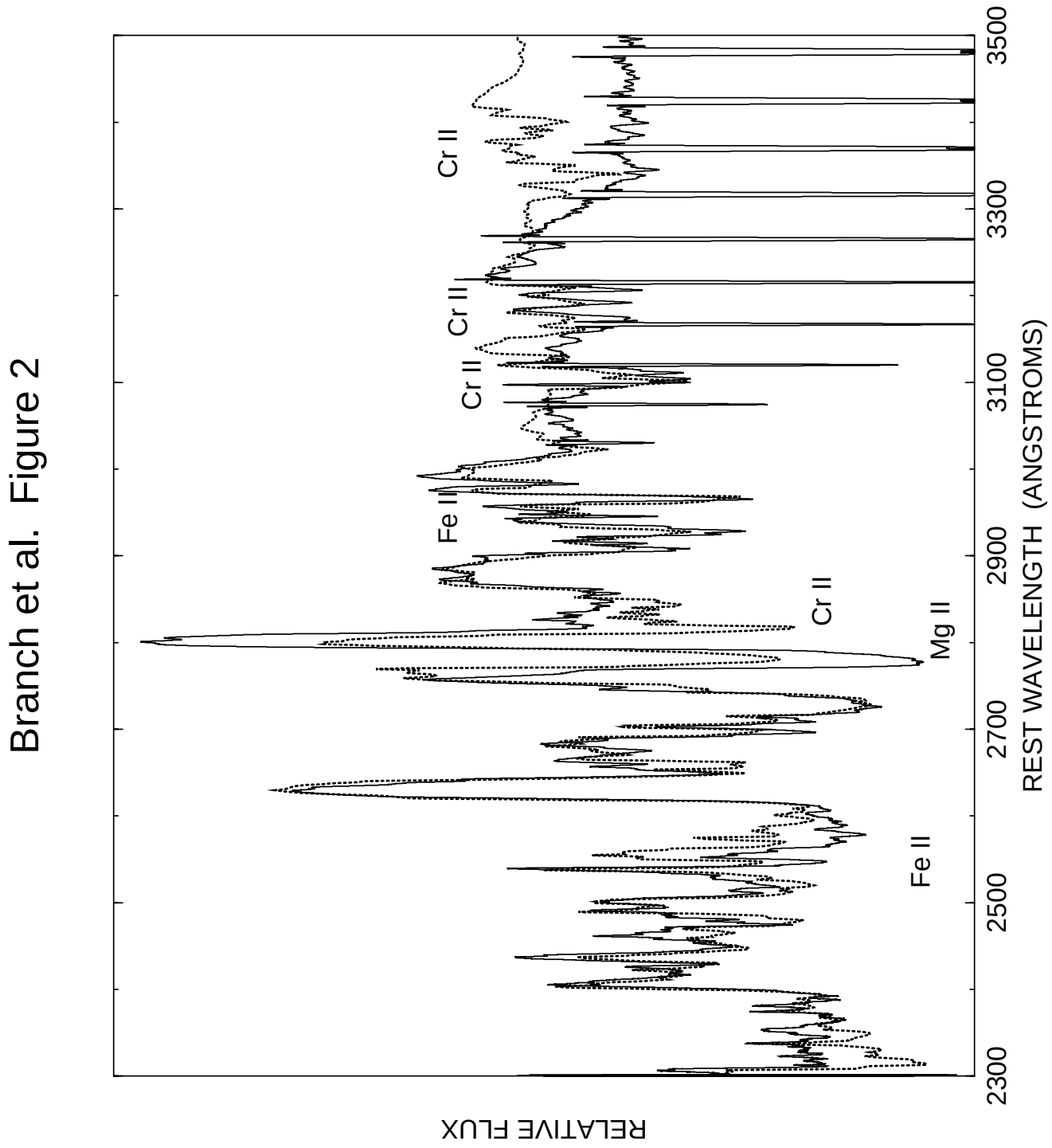

Fig. 2.— The spectrum of FBQS 1214+2803 (*solid line*) is compared with a resonance–scattering synthetic spectrum (*dotted line*) that contains lines of Mg II having $v_{min} = 1000$ km s^{-1} and $v_{max} = 2800$ km s^{-1}, and lines of Fe II and Cr II having $v_{min} = 1800$ km s^{-1}. Fe II dominates the spectrum to the left of the Mg II absorption. The 10 narrow symmetric dips in the observed spectrum are gaps in the echelle orders and have nothing to do with the spectrum of FBQS 1214+2803.

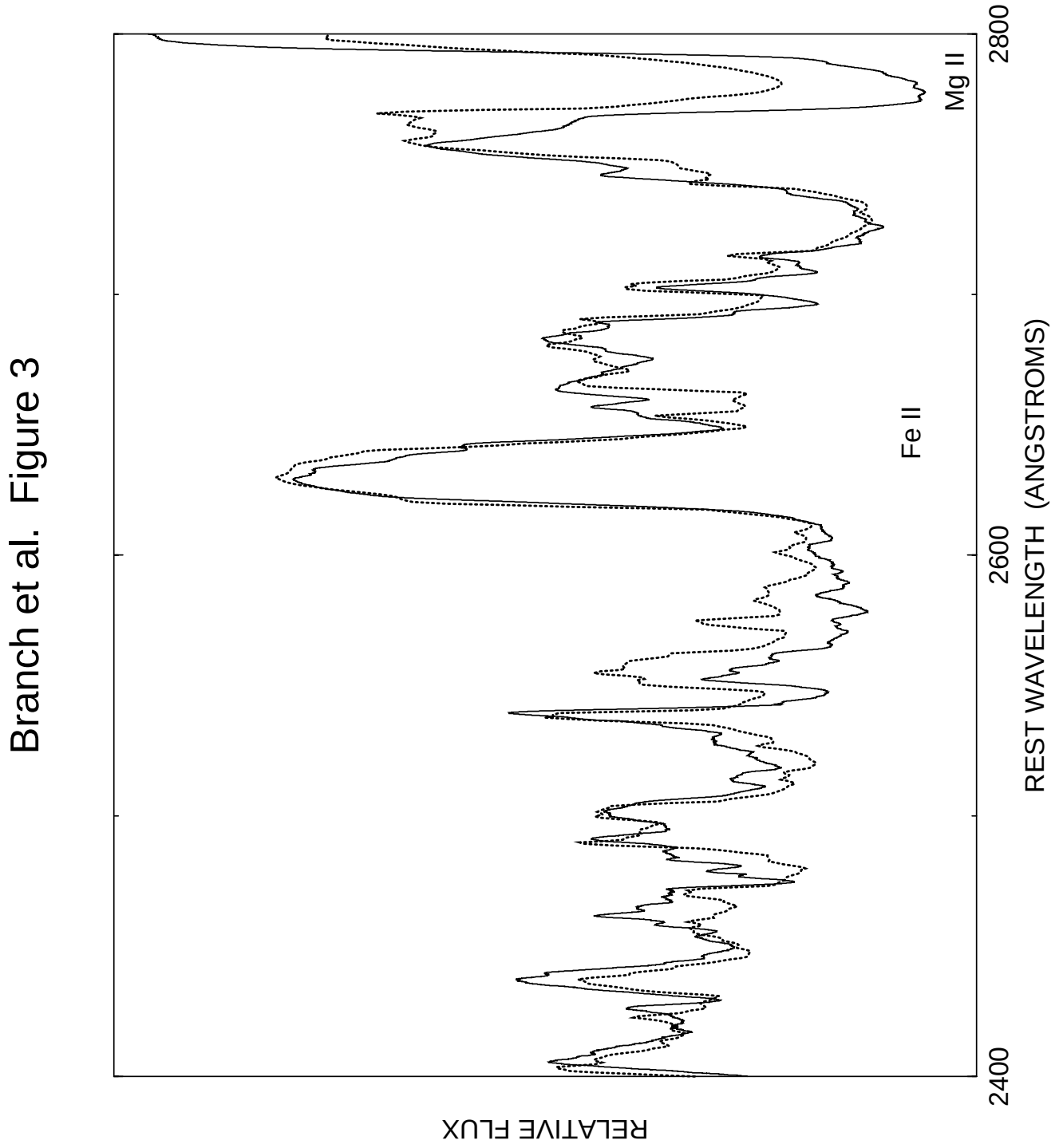

Fig. 3.— A closer look at a crowded part of the observed and synthetic spectra of Fig. 2. Fe II dominates the spectrum to the left of the Mg II absorption.